Chem. Pap. (2017) 71:127–135
DOI 10.1007/s11696-016-0070-y

ORIGINAL PAPER

Application of chemometric methods to the purity analysis of PAMAM dendrimers

Ali S. Ertürk[1] · Abdürrezzak E. Bozdoğan[2] · Metin Tülü[2]

Received: 24 March 2016 / Accepted: 4 August 2016 / Published online: 7 December 2016

Abstract Developing analytical or instrumental methods for the purity assessment of poly(amidoamine) dendrimers (PAMAMs) is almost equally important as much as integrating novel synthesis and purification methods to obtain ideal and monodisperse dendrimers. The aim of this study was to investigate the use of chemometric methods; principal component regression (PCR), and partial least squares (PLS2) to assess the purity of PAMAMs. A full factorial experimental design was used to construct PCR and PLS2 calibration models. Absorbance spectra of PAMAMs were collected by UV–Vis spectroscopy between the wavelength ranges of 250–350 nm with 1.00 nm intervals at 101 points. PCR and PLS2 multivariate models were constructed from these full spectra. The built models were compared in terms of prediction powers by means of relative mean square error of prediction values. Validation results of these models provided compelling evidence that PCR and PLS2 models, indeed PLS2 better, could be successively used to predict PAMAM mixtures quantitatively and qualitatively in terms of components. The developed models could be used to assess the purity of PAMAMs successfully for routine laboratory analysis in future studies.

Keywords PAMAM dendrimers · Chemometric methods · UV–Vis spectroscopy · Simultaneous separation of binary mixtures · Purity assessment

✉ Ali S. Ertürk
aserturk@adiyaman.edu.tr; aserturk@gmail.com

[1] Department of Basic Pharmaceutical Sciences, Faculty of Pharmacy, Adıyaman University, 02040 Adıyaman, Turkey

[2] Department of Chemistry, Yıldız Tehcnical University, 34210 Istanbul, Turkey

Introduction

Over the past decades, dendrimers have been attractive for a number of different applications due to their well-defined, monodisperse, three-dimensional, and hyperbranched starbust structures. In particular, poly(amidoamine) PAMAM dendrimers have received much attention as candidates for various therapeutic, biomedical, and diagnostic applications containing intracellular and targeted drug-delivery, gene delivery, and diagnostic imaging (Pourianazar et al. 2014; Kesharwani et al. 2014; Wang et al. 2016; Parisi et al. 2016; Mekuria et al. 2016). PAMAMs are methodically constructed through either divergent or convergent synthesis. In the divergent synthesis, repetition of the alkylation and amidation steps iteratively yields to next higher generation. The controlled convergent synthesis of PAMAMs leads to well-defined molecular masses. Although PAMAMs can have polydispersity indices as low as 1.01, using classical divergent and convergent synthetic methods gives mixtures of products, by-products, branching defects, and lower generations (trailing generations) (Tolić et al. 1997; van Dongen et al. 2013; Islam et al. 2005). The presence of impurities and trailing generations leads to heterogeneity and requires intense and careful purification to prepare PAMAMs for use in many of the referenced applications.

Purification of dendrimers is an important goal to be achieved as much as obtaining higher yield and ideal growth because of the heterogeneity of the dendrimers is expected to influence the material properties, such as water solubility and biodistribution (Almeida et al. 2011). In particular, the choice of core, repeating units, and surface functional groups can be substantially significant on the overall physical and chemical characteristics of the dendrimers (Scott et al. 2004). Several groups reported defects

and trailing generations leading to the structural heterogeneity arising during the dendrimer synthesis (Peterson et al. 2003; Tomalia et al. 1990; Kallos et al. 1991; Tolić et al. 1997). A recent research indicates that membrane dialysis improves the uniformity of commercially available PAMAMs (Mullen et al. 2012). In addition, liquid-phase retention (LPR) (Spivakov et al. 1985) can be used for the removal of these heterogeneities as an advanced technique. Therefore, these materials can reach the desired purity to be used as a proper sample in nonviral gene delivery mechanic, polycationic–cellular membrane interaction, target delivery, and molecular imaging studies (Mullen et al. 2012). In summary, the ideal and monodisperse dendrimer synthesis, which is important in terms of the application field where the dendrimer will be utilized, can be possible by the use of proper synthesis and purification methods together (Ertürk et al. 2014, 2015).

Up to present, several instrumental methods, such as LC, MS, and CE, have been applied to detect evolving unpurified lower generations (trailing generations) (Li et al. 2000; Peterson et al. 2002; Shi et al. 2005; Caminade et al. 2005; Baytekin et al. 2006; Giordanengo et al. 2007; Pande and Crooks 2011). However, these analytical methods are mostly expensive or not always pervious for the routine laboratory analysis. Furthermore, validation of these methods might require long effort or pretreatments depending on the sample matrix in each generation. To the best of our knowledge, no analytical techniques have been proposed for the quantification of dendrimers in the mixtures until now. Therefore, it will be important to develop fast, simple, and low-cost analytical techniques for the determination and purity assessment of dendrimer generations.

Multivariate chemometric methods (Joliffe and Morgan 1992; Martens 1991; Martens and Martens 2000), such as principal component regression (PCR) and partial least squares (PLS2), help to analyze analytical information from full spectra. Moreover, multivariate chemometric tools have widely been used in the simultaneous qualification and quantification of mixtures (Kumar et al. 2014), and could be an alternative for the purity assessment of dendrimers. PCR and PLS2 have been attracting increasing attention as multivariate calibration methods for the multicomponent analysis of mixtures (Martens and Naes 1989; Brereton 2003; Brown and Ferré 2009). These techniques are useful for analyzing mixtures of components that show strongly overlapping spectra, and allow the rapid and simultaneous determination of each component with minimum sample preparation, reasonable accuracy, precision, and without need of time-consuming separations.

Principles component analysis based methods do not require the spectra or concentrations of all compounds in a mixture. In these methods, it is important to make a sensible estimate of significant components characterizing a mixture. PCR uses regression to convert principle component scores to concentrations (Martens and Naes 1989; Brereton 2003).

PLS considers errors in both the concentration estimates and the spectra, whereas PCR assumes that the concentration estimates are error free. PLS attempts to find factors, called latent variables, that maximize the amount of variation in spectra that are relevant for predicting concentrations, whereas, in PCR, the factors, called principal components, are selected based on the amount of variation that they explain in variables. PLS2 is the extension of PLS1. In PLS1, one compound is modelled at a time, whereas in PLS2, all known compounds can be included in the model (Martens and Naes 1989; Brereton 2003; Brown and Ferré 2009; Wise et al. 2006).

The purpose of this study is to describe and examine the application of the multivariate chemometric calibration methods PCR and PLS2 for the purity assessment of PAMAMs. For this purpose, a full factorial experimental design was used to develop PCR and PLS2 models. Developed models were applied to evaluate the purity of binary mixtures of PAMAMs both quantitatively and qualitatively from UV–Vis spectroscopic data. The models were compared in terms of root-mean-square errors. The validation of the developed models demonstrated that PCR and PLS2 models could be successfully used to predict concentrations of dendrimer mixtures simultaneously and take part of the routine laboratory purity assessment of dendrimers in future studies without using any pretreatment due to the sample matrix.

Experimental

Materials

Jeffamine® T-403, Mn 440 was purchased from Aldrich. Methyl acrylate, ethylenediamine, *n*-butanol, and methanol were purchased from Merck. Unless it was stated, all other chemicals were analytical grade and used directly without purification. LPR ultrafiltration membranes, Amicon 8000 stirred cell, and dialysis membranes, which have the molecular cut of size (MWCO) 0.5, 1 and 3 kDa, were supplied from Millipore. Double distilled 18.2 MΩ cm Milli-Q deionized (Millipore) water was used for LPR experiments.

Instrumentation

The CEM Focused Microwave™ Synthesis System, Model Discover (CEM Corporation, North Carolina, USA) with a continuous microwave power delivery system with the

operator selectable power output from 0 to 300 W (±30 W) programmable in 1-W increments, infrared temperature control system programmable from 25 to 250 °C, and 5 to 125 mL vessel capacity was used as microwave reactor. UV–Vis spectra were obtained using a PG T 70 Spectrometer (PG Instruments, England) with a quartz cuvette cell which has an optical path length of 1.00 cm. Double distilled 18.2 MΩ cm Milli-Q deionized (Millipore) water was used for background subtraction. Eigenvector Research Chemometric Software, Solo+MIA 7.03 (Solo with Multivariate Image Analysis built-in), was used for PCR and PLS2 calibrations.

Microwave assisted synthesis of Jeffamine® T-403 cored PAMAMs

PAMAMs, generation 2 (P_2) and 3 (P_3), were synthesized according to our recently reported method (Ertürk et al. 2014) and briefly summarized hereafter. This method involves alkylation and amidation steps. In the alkylation step, excess methyl acrylate (2.5 M eq. per terminal amine) was added to a methanolic solution of commercially available Jeffamine® T-403 polymer. The reaction mixture was stirred for 24 h at room temperature. Excess reagents and solvents were removed under vacuum at 65 °C bath temperature and purified by LPR. The resulting half-generation ester terminated product $P_{0.5}$ was colorless oil (93%). In amidation, excess ethylenediamine (EDA) (10 M eq.of EDA per ester branched half generation) was added to the stirred methanolic solution of $P_{0.5}$. The final mixture was irradiated with microwave (MW) at 200 W for 30 min. Final traces of EDA were removed under vacuum below the bath temperature of 65 °C using 50 mL of *n*-butanol as hydrogen competitive reagent for three times. The final product was purified by LPR. The resulting product was full-generation amine terminated P_1 (92%). By repeating the above cycle, syntheses of desired PAMAM generations, P_2 and P_3, were performed (Fig. 1).

Purification of PAMAMs: liquid-phase polymer retention technique (LPR)

LPR has the principle of separation of small molecules or fractals from high-molecular weight macromolecules by means of ultrafiltration membranes. When water-soluble macromolecule solutions are placed into LPR system and diafiltered through a membrane, the membrane retains the molecules with the higher molecular weights compared to its molecular weight cut of size (MWCO) and permeates the smaller ones. Dendrimers with the higher molecular weight should be dialyzed with membranes of low MWCO to be sure about the purification of the dendrimer from fragmental and reagents. PAMAMs, P_2 and P_3, were purified in the principle of the LPR and then characterized. The main components of LPR system are a filtration unit (a stirred cell), a membrane filter with appropriate MWCO size, and a pressure source (N_2) gas. Detailed systematic explanations and applications of LPR can be found in the literature (Spivakov et al. 1985; Rivas and Geckeler 1992), but the ideal one can be considered as a continuous flow LPR system (Rivas et al. 2011).

Appropriate Millipore ultrafiltration membrane disk was equipped with Amicon 8000 stirred cell. (1:1) MeOH:aqueous solutions of crude product were transferred into the cell. Depending on the expected size of the product, membrane disks were selected in the range of MWCO 1–3 kDA. The solution was diluted to 200 mL inside the cell. Methanol–water mixture was used as feeding solvent. Continuous dialysis was performed under 15 psi nitrogen pressure for 24 h. Finally, the methanol water mixture was evaporated under vacuum.

Preparation of dendrimer solutions

Aqueous solutions of intensively LPR purified PAMAMs, P_2, and P_3, were used to prepare the binary mixtures of calibration samples C1–C9 (Table 2) and validation set (Table 3). 18.2 mΩ cm double distilled Milli-Q water was used to prepare solutions. No any other sample preparations and treatments were performed before the UV–Vis spectroscopy analysis.

Design and analysis of experiments: calibration and validation sets

Binary mixtures of Jeffamine® T-403 cored PAMAMs with varying concentrations of LPR purified P_2 and P_3 were analyzed by UV–Vis spectrophotometer. Then, calibration and prediction data sets were constructed. A 3^2 (l^k) full factorial design (Montgomery 2005) was used for the design of experiments to build PCR and PLS2 calibration models. The number of independent variables, Y_1 and Y_2, indicating the P_2 and P_3 ($k = 2$) materials in the mixture, was selected as two. The overall absorbance when each component is at a maximum in the mixture was determined within the Beer−Lambert limit (without exceeding 1.2 AU for safety). The three concentration levels ($l = 3$) corresponding to the values of 0.40, 0.99, and 1.59 g L^{-1} for P_2 and 0.39, 0.97, and 1.55 g L^{-1} for P_3 were selected. Table 1 shows the design variables that are used for composition of the binary mixtures of P_2 and P_3 used in the calibration set. The absorption spectrum of each sample was recorded with 1.00 cm cuvettes between 250 and

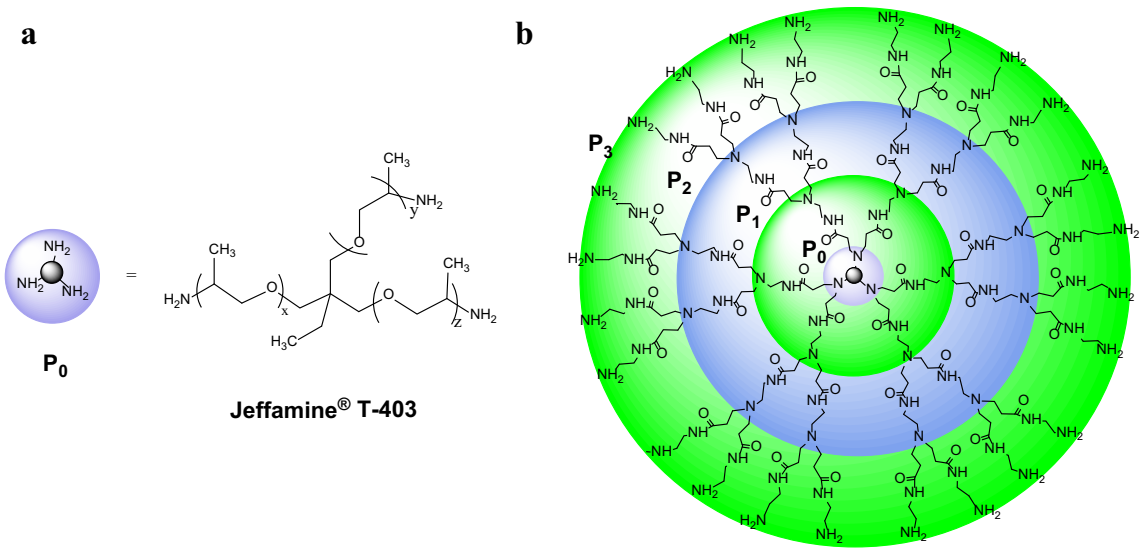

Fig. 1 Jeffamine® T-403 core (**a**) and structure of PAMAMs, generation 2 (P_2), and generation 3 (P_3) (**b**)

Table 1 Design variables and their coded and actual values used for experimental design

Design variable (factor)	Symbols	Actual values of coded levels		
		−1	0	1
P_2 concentration (g L^{-1})	Y_1	0.40	0.99	1.59
P_3 concentration (g L^{-1})	Y_2	0.39	0.97	1.55

350 nm wavelength ranges at 1.00 nm intervals against a blank of 18.2 mΩ double distilled Milli-Q water. Mutually orthogonal designs were constructed by conducting ($l^k = 3^2$) nine experiments (C1–C9) for calibration data (Table 2). UV–Vis spectra of calibration samples C1–C9 were collected between 250 and 350 nm in distilled water

Table 2 3^2 full factorial design and calibration set for P_2 and P_3 mixtures

Batch code	Factors (controllable input variables)			
	Initial P_2 concentration		Initial P_3 concentration	
	P_2 (g L^{-1})	Level Y_1	P_3 (g L^{-1})	Level Y_2
C1	0.40	−1	1.55	+1
C2	1.59	+1	0.97	0
C3	1.59	+1	0.39	−1
C4	0.40	−1	0.97	0
C5	0.40	−1	0.39	−1
C6	0.99	0	0.97	0
C7	1.59	+1	1.55	+1
C8	0.99	0	0.39	−1
C9	0.99	0	1.55	+1

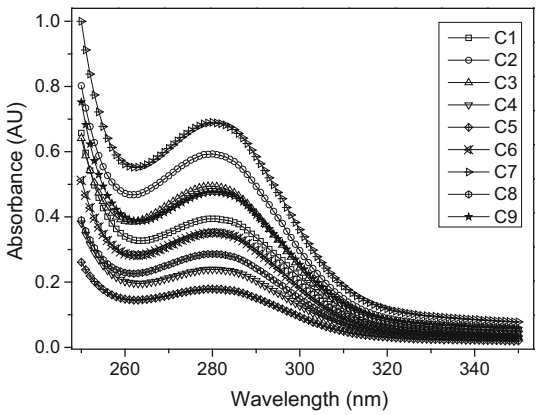

Fig. 2 Full response UV spectra of calibration set C1–C9

as full spectral responses, and all the obtained spectral data in 250–350 nm wavelength range were used to develop multivariate calibration models (Fig. 2).

Data set

UV–Vis spectra of PAMAMs, P_2 and P_3, mixtures were collected between the wavelength range of 250–350 nm, which are including the λ_{max} absorbance values of P_2 and P_3. Spectral evaluation and all preprocessing of data involving centering and normalization were performed by Solo+MIA 7.0.3 (Solo with Multivariate Image Analysis built-in.) Eigenvector Research Software. After the pre-processing, data were divided into a calibration set C1–C9 (nine samples) (Table 2) to build the model and a test set (seven samples) to validate the model. Thus, data set including 16 spectrums was obtained. Finally, PCR and

Table 3 Validation set for P_2 and P_3

Sample number	P_2 (g L^{-1})	P_3 (g L^{-1})
1	0.58	0.49
2	0.77	0.65
3	0.96	0.81
4	1.15	0.97
5	0.79	0.91
6	0.99	1.13
7	1.12	1.36

PLS2 regression methods were used to develop multivariate calibration models (Table 3).

Variable selection

The real reason to build regression models was to make predictions of P_2 and P_3 quantities of PAMAM dendrimer mixtures, simultaneously. Therefore, before considering the predictive abilities of the models, the first thing to be focused on is the root-mean-square error of calibration (RMSEC). It is defined as

$$\mathrm{RMSEC} = \sqrt{\sum_{i=0}^{C} \frac{(\hat{y}_i - y_i)^2}{C}}, \quad (1)$$

where $\hat{y}_i$ are the values of the predicted variable when all samples are included in the model formation and C is the number of the calibration samples. RMSEC is the measure of how well the model fits the data.

The ability of the model to predict samples that were not used to build the model is referred as the root-mean-square error of cross validation (RMSECV). Equation (1) can also be used for the calculation of the RMSECV. In this case, $\hat{y}_i$ corresponds to predictions for samples that were not included in the model formation. To determine the number of factors (k) to be used in PCR and PLS2, cross-validation procedure was used. In this procedure, ith sample of the data set is left out once, and the remaining samples, PCR and PLS2 models, are formed (Şahin et al. 2012). RMSECV usually refers to cross-validation experiments where the calibration data set is divided into two groups as training and test sets to evaluate how a calibration data would perform when applied to a new data. In addition to this, this evaluation can be performed directly by applying a completely independent prediction set of samples that have known Y values. In this point, root-mean-square error of prediction (RMSEP) can be calculated when the model is applied to a new data. RMSEP can be calculated as

$$\mathrm{RMSEP} = \sqrt{\sum_{i=0}^{C_t} \frac{(\hat{y}_i^t - y_i^t)^2}{C_t}}, \quad (2)$$

where C_t is the number of test sets; $\hat{y}_i^t$ and y_i^t indicate the measured value and predicted value from the model for ith sample.

Results and discussions

UV–Vis spectroscopy analysis of PAMAMs

PAMAMs can show maximum UV absorption band depending on their internal tertiary amines. These bands can be observed in different wavelength ranges according to generations. Pande and Crooks (2011) reported these characteristic bands between the wavelength range of 280–285 nm. We have also observed these characteristic UV absorption bands (Fig. 3) for Jeffamine® T-403 cored PAMAMs in our recent study (Ertürk et al. 2014) as in good agreement with the literature (Pande and Crooks 2011). Figure 3 shows the individual UV–Vis absorption spectrums of P_2 (285 nm), P_3 (280 nm), and mixtures. It exists approximately 5 nm maximum absorption band difference between the individual spectrums of P_2 and P_3. This small difference makes difficult to identify, screen, and quantify the binary mixtures of P_2 and P_3. However, it could be possible by developing multivariate calibration models based on the full factorial experimental design (Montgomery 2005). Furthermore, full UV–Vis spectra of the binary mixtures may convey the large scale of information. Chemometric models (PCR and PLS2) could be used to interpret and evaluate these full spectra as a response matrix. Thus, the P_2 and P_3 concentrations from the binary mixtures of Jeffamine® T-403 cored PAMAMs could be predicted simultaneously.

In UV–Vis assays, 250–350 nm full range of UV spectra was used to collect information for the development of multivariate calibration models (Fig. 2). In this range,

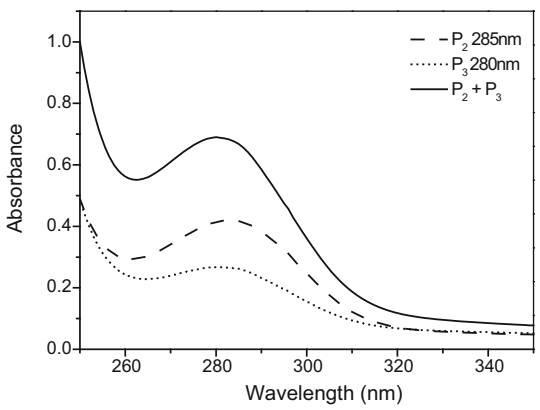

Fig. 3 Absorption spectra of aqueous 1.59 g L^{-1} P_2, 1.55 g L^{-1} P_3 solutions, and mixture ($P_2 + P_3$) of them

280–285 nm band characteristic to PAMAMs for P_2, P_3 solutions and binary mixture ($P_2 + P_3$) of them were observed successfully (Fig. 3). Then, this range was used in a good agreement to model calibration data (C1–C9), which is designed with 3^2 full factorial design (Table 2). C1–C9 calibrations samples were prepared from the LPR purified P_2 and P_3 dendrimers. Absorbance spectrum of each calibration sample (C1–C9) refers to overlapped mixture absorbance spectra of the P_2 and P_3 dendrimer solutions. Thus, the observed absorbance spectra in Fig. 2 between 270 and 290 nm origin from the overlapping characteristic dendrimer peaks stemming from the absorbances of the internal tertiary amine groups of P_2 and P_3 at around 280–285 nm.

Design of experiments and data processing

Spectroscopic data can be designed in $m \times n$ data matrix X, where m refers the number of calibration experiments (C1–C9) and n indicates the number of variables (wavelengths: 250–350 nm). In this study, calibration experiments were conducted by applying 3^2 full factorial design. Thus, nine experiments were conducted at three levels for the simultaneous determination of P_2 and P_3 from binary dendrimer mixtures (Table 2). UV spectra of each calibration experiment were collected between 250 and 350 nm and absorbance values at each wavelength were used to construct $X_{m\times n}$ data matrix (response-full spectra matrix). On the other hand, $Y_{m\times 2}$ concentration matrix was constructed using actual values instead of coded values of Y_1 and Y_2 variables illustrated in Tables 1 and 2. Precision and prediction ability of chemometric models can be influenced by preprocessing. Hence, preprocessing of normalization and column centering were applied both to the X and Y matrices by Solo MIA 7.0.3 Eigenvector Software auto-scaling function.

Determination of the number of variables

The UV spectra of P_2 (1.59 g L^{-1}) and P_3 (1.55 g L^{-1}) are shown in Fig. 3. As it can be seen from Fig. 3, direct spectrophotometric determination of one generation in the presence of second one is impossible due to the strong overlapping spectra of them. Therefore, PCR and PLS2 calibration methods were applied to resolve the overlapped mixture spectra of two dendrimer generations, P_2 and P_3.

Absorption spectra for the standard samples (C1–C9) shown in Table 2 were recorded in the range of 250–350 nm at 101 points and subjected to PCR and PLS2 analysis. In these methods, calibration was performed using the absorbance ($X_{m\times n}$) and concentration matrices ($Y_{m\times 2}$) to predict the unknown concentrations of the dendrimer generations from their binary mixtures. PLS2 and PCR models require to determine the optimal number of principal components (PCs) or latent variables (LVs) before the calibration models are constructed. The optimum number of PCs and LVs was determined by applying cross-validation procedure (Brereton 2003). In this procedure, *i*th sample of the data leaves one out once, and PCR and PLS2 models have been built. The root-mean-square error of cross validation (RMSECV) was used as the statistical parameter to obtain the optimum number of PCs and LVs. This parameter is defined in Eq. (1). PCR and PLS2 models require the optimal number of PCs or LVs when the local minimal level of RMSEC is reached. In fact, a good rule to decide the number of components is not to include additional factors improving the RMSECV at least 2%. It can be obviously seen from Fig. 4 that PCs and LVs in PCR and PLS2 models do not improve more than 2% at the local minima of three PCs or LVs for both P_2 and P_3. In addition, it is more reliable to construct a model with less complexity. For these reasons, PCs and LVs to build the PCR and PLS2 models were selected as three as it is marked with the circle (Fig. 4).

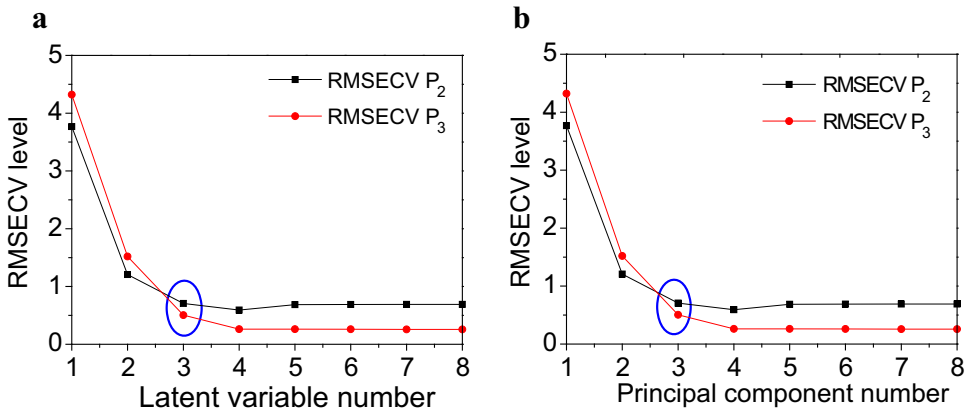

Fig. 4 RMSECV versus LV for PLS2 (**a**) and RMSECV versus PC for PCR (**b**) on calibration data

Table 4 Comparison of RMSEC, RMSECV, and RMSEP on PCR and PLS2 models

Model	P_2				P_3			
	RMSEC	RMSECV	RMSEP	R^2	RMSEC	RMSECV	RMSEP	R^2
PLS2	0.29	0.71	0.23	0.9965	0.25	0.50	0.32	0.9974
PCR	0.28	0.70	0.47	0.9968	0.28	0.54	0.35	0.9966

Comparison of chemometric methods: principal component regression (PCR) and partial least squares (PLS2)

In the divergent synthesis of PAMAMs, core monomer or polymer is reacted with successive addition of excess methyl acrylate and ethylene diamine for the synthesis of higher generation dendrimers. Insufficient or improper purification of the synthesized dendrimers results in non-ideal lower generation growth (Mullen et al. 2012). In this point, multivariate calibration models could be used as a purity or ideal structural growth screening tools. Therefore, the components of the dendrimer solutions can be determined quantitatively. Table 4 illustrates the comparison of PCR and PLS2 models from the aspect of prediction powers. In Table 4, it can be clearly seen that RMSEC, the error of calibration, values for P_2 and P_3 are ranged between 0.25 and 0.29, and PLS2 model shows the smallest RMSEC value for P_3 (0.25) and other RMSEC values cannot be distinguished from each other. In other words, the ability of PCR and PLS2 models to fit calibration data (R^2) for P_2 and P_3 seems to be very close to each other. Furthermore, RMSECV values for P_2 are not a distinguishable value to infer which model predicts best as they have almost the same RMSECV values. On the other hand, one can see from RMSECV values of P_3 that PLS2 has the smallest RMSECV, and it is expected to predict best with the original calibration data. Nevertheless, for the prediction of new samples: validation data (RMSEP), PLS2 model outperforms the other models, and this is followed closely by PCR for P_2. Furthermore, PCR and PLS2 could predict new sample in the same performance as it can be seen the RMSECV values of P_3 (Table 4). In practice, it could be evident from the comparison of models that fit and prediction are totally different aspects of model's performance. When the relative mean standard error prediction (RMSEP) values for PCR and PLS2 in Table 4 are investigated, it can be seen that PLS2 almost predicts better the P_2–P_3 binary dendrimer mixtures with just below the 5 nm maximum absorbance wavelength difference (Fig. 3) in contrast to PCR if prediction is the goal.

Validation

Validation of PCR and PLS2 chemometric models was conducted by selecting seven independent validation test data. Predictive abilities of these models on both calibration and validation data were investigated. *Y* measured and *Y* predicted concentration values for PCR and PLS2 models were shown in Fig. 5. %Residual errors of prediction values of models were calculated. These values were plotted against the total sample number (nine for full factorial calibration data and seven for validation data) (Fig. 5b, d, f, h). Furthermore, 1:1 line and fitting line corresponds to calibration and validation data, respectively. Investigation of the predictive abilities of PCR and PLS models (Fig. 5a, c, e, g) reveals that these models have close regression coefficients to each other [PCR: P_2 ($R^2 = 0.993$), P_3 ($R^2 = 0.995$); PLS2: P_2 ($R^2 = 0.995$), P_3 ($R^2 = 0.995$)], representing both the calibration and validation data. In addition, it could be easily interpreted from the visual data presented in Fig. 5 for the PCR and PLS2 models that 1:1 calibration and validation test set fitting lines are almost overlapped. That is, the PCR and PLS2 models can both predict the calibration data and validation data in reasonable %residual errors. While the PCR model predicts binary mixtures of the PAMAMs between %residual errors of ±8% (RMSEP: $P_2 = 0.698$; $P_3 = 0.535$), PLS2 predicts between those of ±6% (RMSEP: $P_2 = 0.470$; $P_3 = 0.347$). To sum up, the PLS2 predicts better than PCR and both of these methods could be successfully used for the quantitative determination of the binary mixtures of the PAMAMs.

Conclusions

Chemometric analysis of the experimental data designed with 3^2 full factorial experimental design from full spectra can convey large scale of information for the construction of multivariate chemometric models. Hence, data analysis and interpretation could be performed with good reliability and security. Modelling from full spectra can make multivariate calibration models superior as they convey more information compared to simple linear models. In this study, PCR and PLS2 calibration models were constructed to determine the concentration of P_2 and P_3 from binary mixtures of Jeffamine® T-403 cored PAMAMs. The built models were compared in terms of RMSEC, RMSECV, and RMSEP values. Results revealed that developed PCR and PLS2 models could be successfully used for the

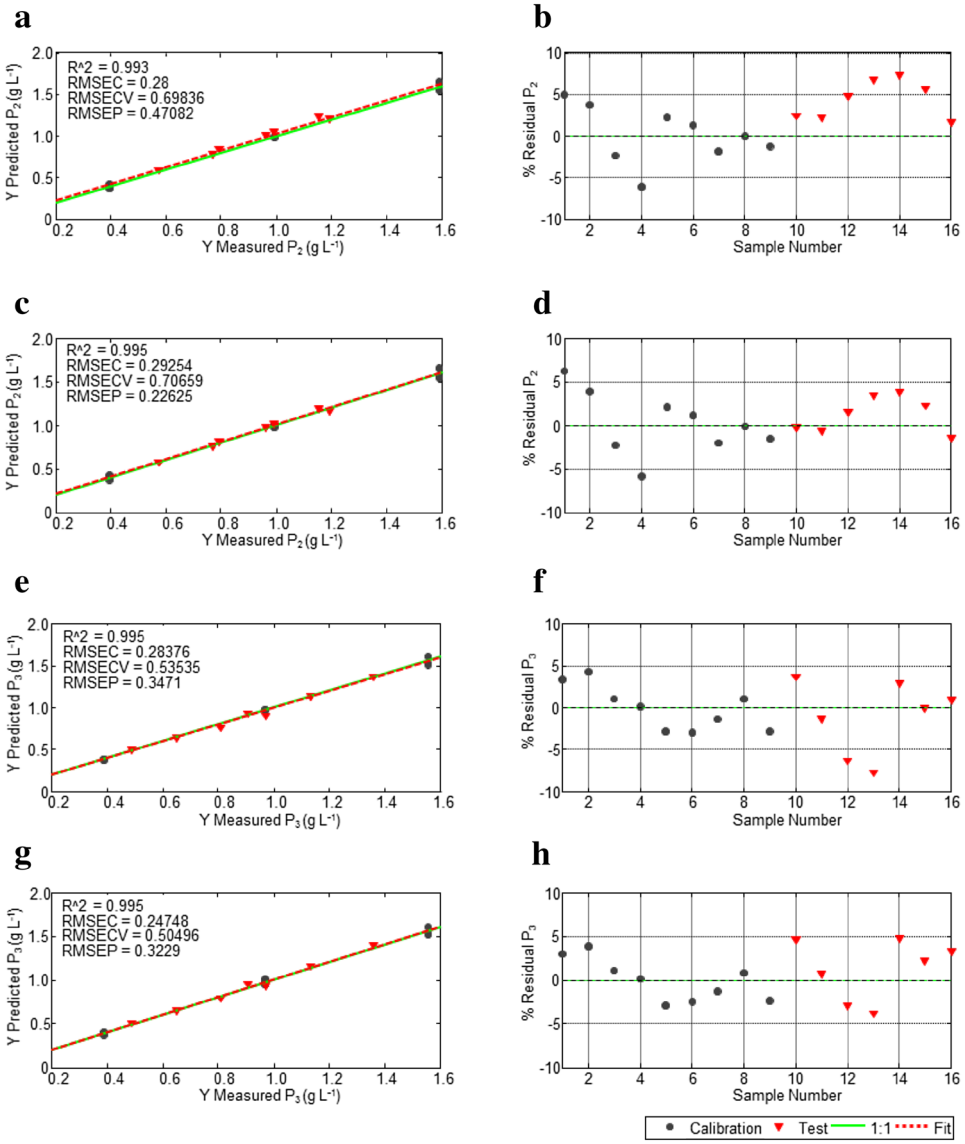

Fig. 5 *Y* measured and predicted values and %residuals of (**a**, **b**) PCR and (**c**, **d**) PLS2 models for P_2 component; *Y* measured and predicted values of (**e**, **f**) PCR, (**g**, **h**) PLS2 models for P_3 component

simultaneous determination of the binary mixtures of PAMAMs from spectroscopic UV–Vis data in routine laboratory analysis. Indeed, PLS2 predicts better. Moreover, these models could be applied for the purity assessment of PAMAMs.

In conclusion, this paper is the first study concerning the purity assessment of PAMAMs using chemometric methods—PCR and PLS2. Thus, the developed models could be easily used in routine laboratory UV–Vis spectroscopy analysis of dendrimer mixtures without using any sample pretreatment in a short time, and for the screening of the dendrimer synthesis.

Acknowledgements This research has been supported by Yıldız Technical University Scientific Research Projects Coordination Department, Project Numbers (2011-01-02-KAP04, 2011-01-02-KAP05, 2011-01-02-KAP06, and 2012-01-02-DOP05).

Compliance with ethical standards

Conflict of interest The authors declare that there is no conflict of interest or competing financial interest related to the work described

References

Almeida JPM, Chen AL, Foster A, Drezek R (2011) In vivo biodistribution of nanoparticles. Nanomedicine (London, UK) 6:815–835. doi:10.2217/nnm.11.79

Baytekin B, Werner N, Luppertz F, Engeser M, Brueggemann J, Bitter S, Henkel R, Felder T, Schalley CA (2006) How useful is mass spectrometry for the characterization of dendrimers? "Fake defects" in the ESI and MALDI mass spectra of dendritic compounds. Int J Mass Spectrom 249(250):138–148. doi:10.1016/j.ijms.2006.01.016

Brereton RG (2003) Chemometrics: data analysis for the laboratory and chemical plant. Wiley, Oxford

Brown SD, Ferré RT (2009) Comprehensive chemometrics: linear regression modeling, non-linear regression, classification, feature selection, multivariate robust techniques. Elsevier, Oxford

Caminade A-M, Laurent R, Majoral J-P (2005) Characterization of dendrimers. Adv Drug Deliv Rev 57:2130–2146. doi:10.1016/j.addr.2005.09.011

Erturk AS, Gurbuz MU, Tulu M, Bozdogan AE (2015) Water-soluble TRIS-terminated PAMAM dendrimers: microwave-assisted synthesis, characterization and Cu(ii) intradendrimer complexes. RSC Adv 5:60581–60595. doi:10.1039/C5RA11157A

Ertürk AS, Tülü M, Bozdoğan AE, Parali T (2014) Microwave assisted synthesis of Jeffamine cored PAMAM dendrimers. Eur Polym J 52:218–226. doi:10.1016/j.eurpolymj.2013.12.018

Giordanengo R, Mazarin M, Wu J, Peng L, Charles L (2007) Propagation of structural deviations of poly(amidoamine) fan-shape dendrimers (generations 0–3) characterized by MALDI and electrospray mass spectrometry. Int J Mass Spectrom 266:62–75. doi:10.1016/j.ijms.2007.07.002

Islam MT, Shi X, Balogh L, Baker JR Jr (2005) HPLC separation of different generations of poly(amidoamine) dendrimers modified with various terminal groups. Anal Chem 77:2063–2070. doi:10.1021/ac048383x

Joliffe I, Morgan B (1992) Principal component analysis and exploratory factor analysis. Stat Methods Med Res 1:69–95. doi:10.1177/096228029200100105

Kallos GJ, Tomalia DA, Hedstrand DM, Lewis S, Zhou J (1991) Molecular weight determination of a polyamidoamine Starburst polymer by electrospray ionization mass spectrometry. Rapid Commun Mass Spectrom 5:383–386. doi:10.1002/rcm.1290050902

Kesharwani P, Jain K, Jain NK (2014) Dendrimer as nanocarrier for drug delivery. Prog Polym Sci 39:268–307. doi:10.1016/j.progpolymsci.2013.07.005

Kumar N, Bansal A, Sarma GS, Rawal RK (2014) Chemometrics tools used in analytical chemistry: an overview. Talanta 123:186–199. doi:10.1016/j.talanta.2014.02.003

Li J, Piehler LT, Qin D, Baker JR, Tomalia DA, Meier DJ (2000) Visualization and characterization of poly(amidoamine) dendrimers by atomic force microscopy. Langmuir 16:5613–5616. doi:10.1021/la000035c

Martens H (1991) Multivariate calibration. Wiley, Oxford

Martens H, Martens M (2000) Modified Jack-knife estimation of parameter uncertainty in bilinear modelling by partial least squares regression (PLSR). Food Qual Pref 11:5–16. doi:10.1016/s0950-3293(99)00039-7

Martens H, Naes T (1989) Multivariate calibration. Wiley, Oxford

Mekuria SL, Debele TA, Tsai H-C (2016) PAMAM dendrimer based targeted nano-carrier for bio-imaging and therapeutic agents. RSC Adv. doi:10.1039/C6RA12895E

Montgomery DC (2005) Design and analysis of experiments, student solutions manual. Wiley, Oxford

Mullen DG, Desai A, van Dongen MA, Barash M, Baker JR Jr, Banaszak Holl MM (2012) Best practices for purification and characterization of PAMAM dendrimer. Macromolecules 45:5316–5320. doi:10.1021/ma300485p

Pande S, Crooks RM (2011) Analysis of poly(amidoamine) dendrimer structure by UV–vis spectroscopy. Langmuir 27:9609–9613. doi:10.1021/la201882t

Parisi OI, Scrivano L, Sinicropi MS, Picci N, Puoci F (2016) Engineered polymer-based nanomaterials for diagnostic, therapeutic and theranostic applications. Mini Rev Med Chem 16:754–761. doi:10.2174/1389557515666150709112122

Peterson J, Allikmaa V, Subbi J, Pehk T, Lopp M (2002) Structural deviations in poly(amidoamine) dendrimers: a MALDI-TOF MS analysis. Eur Polym J 39:33–42. doi:10.1016/S0014-3057(02)00188-X

Peterson J, Allikmaa V, Subbi J, Pehk T, Lopp M (2003) Structural deviations in poly(amidoamine) dendrimers: a MALDI-TOF MS analysis. Eur Polym J 39:33–42. doi:10.1016/s0014-3057(02)00188-x

Pourianazar NT, Mutlu P, Gunduz U (2014) Bioapplications of poly(amidoamine) (PAMAM) dendrimers in nanomedicine. J Nanopart Res. doi:10.1007/s11051-014-2342-1

Rivas B, Geckeler K (1992) Synthesis and metal complexation of poly(ethyleneimine) and derivatives. Polymer synthesis oxidation processes. Advances in polymer science, vol 102. Springer, Berlin, pp 171–188. doi:10.1007/3-540-55090-9_6

Rivas BL, Pereira ED, Palencia M, Sánchez J (2011) Water-soluble functional polymers in conjunction with membranes to remove pollutant ions from aqueous solutions. Prog Polym Sci 36:294–322. doi:10.1016/j.progpolymsci.2010.11.001

Şahin S, Işık E, Demir C (2012) Prediction of total phenolic content in extracts of Prunella species from HPLC profiles by multivariate calibration. ISRN chromatography 2012

Scott RWJ, Wilson OM, Crooks RM (2004) Synthesis, characterization, and applications of dendrimer-encapsulated nanoparticles. J Phys Chem B 109:692–704. doi:10.1021/jp0469665

Shi X, Banyai I, Islam MT, Lesniak W, Davis DZ, Baker JR, Balogh LP (2005) Generational, skeletal and substitutional diversities in generation one poly(amidoamine) dendrimers. Polymer 46:3022–3034. doi:10.1016/j.polymer.2005.01.081

Spivakov BY, Geckeler K, Bayer E (1985) Liquid-phase polymer-based retention—the separation of metals by ultrafiltration on polychelatogens. Nature (London) 315:313–315. doi:10.1038/315313a0

Tolić LP, Anderson GA, Smith RD, Brothers HM, Spindler R, Tomalia DA (1997) Electrospray ionization Fourier transform ion cyclotron resonance mass spectrometric characterization of high molecular mass Starburst^{TM} dendrimers. Int J Mass Spectrom Ion Processes 165:405–418. doi:10.1016/S0168-1176(97)00161-4

Tomalia DA, Naylor AM, Goddard WA (1990) Starburst dendrimers: molecular-level control of size, shape, surface chemistry, topology, and flexibility from atoms to macroscopic matter. Angew Chem Int Ed 29:138–175. doi:10.1002/anie.199001381

van Dongen MA, Desai A, Orr BG, Baker JR Jr, Banaszak Holl MM (2013) Quantitative analysis of generation and branch defects in G5 poly(amidoamine) dendrimer. Polymer 54:4126–4133. doi:10.1016/j.polymer.2013.05.062

Wang H, Huang Q, Chang H, Xiao J, Cheng Y (2016) Stimuli-responsive dendrimers in drug delivery. Biomater Sci 4:375–390. doi:10.1039/c5bm00532a

Wise BM, Gallagher NB, Bro R, Shaver JM, Koch RS (2006) Chemometrics tutorial for PLS toolbox and solo. Eigenvector Research Inc, Wenatchee, p 414